Impaired peri-olfactory cerebrospinal fluid clearance is associated with ageing, cognitive decline and dyssomnia

Ying Zhou,[a,c] Wang Ran,[a,c] Zhongyu Luo,[a] Jianan Wang,[a] Mengmeng Fang,[b] Kai Wei,[b] Jianzhong Sun,[b] and Min Lou[a,]*

[a]Department of Neurology, The Second Affiliated Hospital of Zhejiang University, School of Medicine, Hangzhou, China
[b]Department of Radiology, The Second Affiliated Hospital of Zhejiang University, School of Medicine, Hangzhou, China

Summary

Background Animal experiments have demonstrated the dependency of cerebrospinal fluid clearance function on age and sleep, which partially underlay the cognitive decline in the elderly. However, human evidence is lacking, which could be mainly attributed to the limited methods of cerebrospinal fluid clearance function assessment.

Method Serial T1-weighted and T2-fluid attenuated inversion recovery imaging were performed in 92 patients before and at multiple time points including 4.5 h, 15 h and 39 h after intrathecal injection of contrast agent to visualize the putative meningeal lymphatic pathway, peri-olfactory nerve pathway, and peri-optic nerve pathway. We defined the clearance function as the percentage change in signal unit ratio of critical locations in these pathways from baseline to 39 h after intrathecal injection, and further analysed their relationships with age, sleep, and cognitive function.

Findings Cerebrospinal fluid clearance through the putative meningeal lymphatic and perineural pathways were clearly visualized. The clearance function of putative meningeal lymphatic and perineural pathways were impaired with ageing (all $P < 0.05$). The clearance function through peri-olfactory nerve pathway in inferior turbinate was positively correlated with sleep quality and cognitive function (both $P < 0.05$), and mediated the association of sleep quality with cognitive function (percent change in β [bootstrap 95% CI]: 33% [−0.220, −0.007]).

Interpretation The impaired clearance through putative peri-olfactory nerve pathway may explain the cognitive decline in patients with sleep disturbance. The study shows a promising method to assess cerebrospinal fluid clearance function of putative peri-neural pathways via dynamic magnetic resonance imaging with intrathecal injection of contrast agent.

Funding This work was supported by the National Natural Science Foundation of China (81971101, 82171276 and 82101365).

Keywords: CSF clearance; Intrathecal injection; Cognitive decline; Dyssomnia

Introduction

Cerebrospinal fluid (CSF) is considered to be produced primarily by the choroid plexuses and circulates through the subarachnoid space and ventricles to maintain a stable environment for the brain and spinal cord.[1] Traditionally, it was accepted that CSF mainly drain from the subarachnoid space to the dural venous sinuses through arachnoid granulations.[2] However, this concept has been increasingly challenged in recent years. Accumulating evidences from various species including rodent, artiodactyla and non-human primate have shown that tracers injected into the CSF can be found within lymphatic vessels from the cranium and spine, as well as along exiting cranial and spinal nerves.[3,4] In addition, it is worth noting that several animal studies have found the dependency of CSF clearance function on age, which may partially underlie the cognitive decline in the elderly.[5,6] Additionally, CSF circulation changes under different physiological conditions, for example, drainage of CSF to the deep

*Corresponding author. Department of Neurology, The Second Affiliated Hospital of Zhejiang University, School of Medicine, #88 Jiefang Road, Hangzhou, China.
E-mail addresses: lm99@zju.edu.cn, loumingxc@vip.sina.com (M. Lou).
[c]These authors contribute equally.

Research in context

Evidence before this study
Animal experiments have demonstrated the dependency of cerebrospinal fluid (CSF) clearance function on age and sleep, which partially underlay the cognitive decline in the elderly. However, evidence is lacking in humans mainly due to limited method to assess CSF clearance function.

Added value of this study
Our findings provide in vivo evidence of CSF clearance through peri-olfactory nerve pathway in human by dynamic magnetic resonance imaging (MRI) with intrathecal injection of contrast agent. The clearance function of meningeal lymphatic and peri-neural pathways were reduced with aging.

The clearance function through peri-olfactory nerve pathway mediated the association of sleep quality with cognitive function.

Implications of all the available evidence
In present study, we shows promise for dynamic MRI with intrathecal injection of contrast agent as a method to assess CSF clearance function through putative peri-neural pathways. We demonstrated the potential connection among cognitive function, sleep and CSF clearance function of putative peri-olfactory nerve pathway, which unravel new paradigms and therapeutic directions for cognitive decline induced by sleep disturbed.

cervical and mandibular lymph nodes from the intracranial space is increased when mice are awake compared to anesthesia.[7,8] However, it is still unclear whether the chronic disorders in sleeping pattern could affect CSF drainage.

The meningeal lymphatic vessels were first demonstrated in human using non-invasive high-resolution clinical MRI by Absinta et al.[9] After that, our group and another research group have independently visualized the efflux of intrathecally-administered gadolinium contrast agent to the parasagittal dura, potentially linking CSF in the subarachnoid space to lymphatic vessels in the dura.[10,11] However, the evidences of peri-neural pathways are relatively limited and controversial. A PET study using radionuclide tracers reported nasal turbinate as a location of CSF drainage pathway in healthy human and Alzheimer's disease patients.[12] Conversely, an MRI study found that gadolinium injected into the CSF did not result in significant contrast enhancement detected in the nasal turbinates of patients with normal pressure hydrocephalus.[13] More recently, based on findings in five participants, another MRI study suggested that all peri-neural spaces surrounding cranial nerves were filled with CSF.[14] Collectively, since the existence of peri-neural pathways in humans is still controversial, studies have rarely reported the function of these pathways, or their potential interactions with sleep quality and cognitive function.

In the current study, by utilizing dynamic brain 3-dimensional T1-weighted imaging and high-resolution 2-dimensional T2-fluid attenuated inversion recovery imaging with intrathecal injection of a gadolinium contrast agent, we visualized three main CSF draining pathways including (1) putative meningeal lymphatic pathway through parasagittal dura; (2) putative peri-olfactory nerve pathway through subarachnoid space adjacent to straight gyri and superior, middle, and inferior turbinates; and (3) putative peri-optic nerve pathway through middle intraorbital segment of the optic nerve and corneoscleral part (hereinafter the word

"putative" is omitted, wherever pathway is mentioned). We then assessed the CSF clearance function in each pathway and further investigated their relationships with age, sleep quality, and cognitive function.

Methods
Ethics
The study, including the administration of intrathecal gadolinium agents, obtained approval from the Ethics Committee of Second Affiliated hospital, School of medicine, Zhejiang University (Approval Number: YAN-2018-111). All clinical investigations were conducted in compliance with the principles expressed in the Declaration of Helsinki. Written informed consent was obtained for all the participants.

Experimental design and participants
In this prospective observational study, we enrolled consecutive patients with indications for lumbar puncture and voluntary participation. Exclusion criteria were known adverse reactions to contrast agents, history of severe allergic reactions in general, renal dysfunction, and pregnant or breastfeeding females. All patients underwent MRI before and at multiple time points including 4.5 h, 15 h, and 39 h after intrathecal injection of gadodiamide during a study period from April 2018 to September 2022. The Pittsburgh Sleep Quality Index (PSQI) was used to evaluate the quality and patterns of sleep consisting of seven domains including subjective sleep quality, sleep latency, sleep duration, habitual sleep efficiency, sleep disturbances, use of sleeping medication, and daytime dysfunction for the past month before the first MRI examination in hospital. The total score was 21 with higher scores indicating more severe dyssomnia.[15] The Telephone Montreal Cognitive Assessment (T-MoCA) was used to evaluate the cognitive function consisting of five domains including attention and calculation, language, abstraction, delayed

recall, and orientation one month after discharge over the phone. The total score was 22 points with higher scores indicating better cognitive function.[16]

Intrathecal administration of gadodiamide

The site of intrathecal injection of the contrast agent is L3-4 or L4-5 lumbar intervertebral space. Intrathecal injection of 1 ml of 0.5 mmol/ml gadodiamide (Omniscan; GE Healthcare) was preceded by verifying the correct position of the syringe tip in subarachnoid space in terms of CSF backflow from the puncture needle.[10] Following needle removal, patients were instructed to rotate themselves around the long axis of the body twice, and then remain in the supine position until 4 h after intrathecal injection.

MRI protocol

A 3.0T MRI scanner (GE 750; GE Healthcare, Chicago, IL) with equal imaging protocol settings at all time points was applied to acquire axial head 3-dimensional T1-weighted, high-resolution coronal head 2-dimensional T2-fluid attenuated inversion recovery and axial neck T1 fat-suppression imaging. The main imaging parameters were, for axial head 3-dimensional T1-weighted: repetition time = 7.3 ms, echo time = 3.0 ms, flip angle = 8, thickness = 1 mm, field of view = 25×25 cm^2, matrix = 250×250 pixels; for high-resolution coronal head 2-dimensional T2-fluid attenuated inversion recovery: repetition time = 8400 ms, inversion time = 2000 ms, echo time = 152 ms, flip angle = 90°, thickness = 3 mm, no slice gap, field of view = 18×18 cm^2, matrix = 320×320 pixels; and for neck T1 fat-suppression imaging: repetition time = 535 ms, echo time = 9.1 ms, thickness = 4 mm, slice gap = 0.5 mm, field of view = 22×22 cm^2, matrix = 130×100 pixels.

Evaluation of imaging

A neurologist (R.W.) with 5 years of experience and blind to clinical and other image data independently placed regions of interest (ROIs) at all time points, and performed the image evaluation again six months later in 20 patients for intra-observer consistency, using RadiAnt (Medixant, Poznan, Poland), a Digital Imaging and Communications in Medicine viewer. Another neurologist (Z.Y.) with 10 years of experience and blind to clinical and other image data independently placed ROIs in 20 patients for inter-observer consistency. Different ROIs were placed on different imaging. Specifically, 1) middle intraorbital segment of the optic nerve (hereinafter referred to as the "optic nerve") and corneoscleral part were plotted on axial head 3-dimensional T1-weighted imaging, 2) parasagittal dura, subarachnoid space adjacent to straight gyri (hereinafter referred to as "adjacent straight gyri"),

superior turbinate, middle turbinate and inferior turbinate were plotted on high-resolution coronal head 2-dimensional T2-fluid attenuated inversion recovery imaging, and 3) deep cervical lymph node were plotted on neck T1 fat-suppression imaging. The placements of the ROIs were illustrated in Fig. 1.

We measured mean signal unit for each ROI and normalized them against references. According to previous studies, we chose vitreous body of the ocular bulb on axial head 3-dimensional T1-weighted imaging and high-resolution coronal head 2-dimensional T2-fluid attenuated inversion recovery imaging as references, since there was no significant tracer accumulation in these regions after intrathecal injection of gadodiamide.[13,17] For each time point, we determined the signal unit ratio between the ROIs and references. Examples of placements of reference ROIs were shown in Supplementary Figure S1. We defined the clearance function of each region as the percentage changes in signal unit ratio from baseline to 39 h, with lower percentage changes indicating better clearance function.

In each patient, we compared the signal unit ratio at 4.5 h, 15 h, and 39 h at each region, and the time point of relative high signal unit ratio is defined as the peak time point of CSF tracer enrichment. We then compared the peak time point among different regions, and illustrated them as the tracer appeared at one region before/at the same time point as/later than another region.

Statistical analyses

Continuous data were described as mean with standard deviation or median with interquartile spacing while categorical data were presented as numbers and percentage. Normality was assessed using Shapiro–Wilks normality test. Differences between continuous or categorical data in the same individual were determined using paired-sample t tests or paired-sample Wilcoxon signed rank test, respectively. Correlations between continuous or rank data were determined using Pearson or Spearman correlation analysis, and the Benjamini–Hochberg method was used to correct for multiple comparisons. Multivariable analyses were performed using linear regression analysis. Differences between continuous data were determined using linear mixed models with a random intercept. Bootstrapping technique was used to calculate the empirical power of linear mixed models (10,000 replicate samples with replacement). The inter-observer and intra-observer consistency of the measurements of the percentage changes in signal unit ratio were analysed by interclass correlation coefficient (ICC) in two-way random and absolute agreement model.

Mediation analysis were used to assess whether the association between sleep (PSQI total scores) and cognitive function (T-MoCA total scores) could be
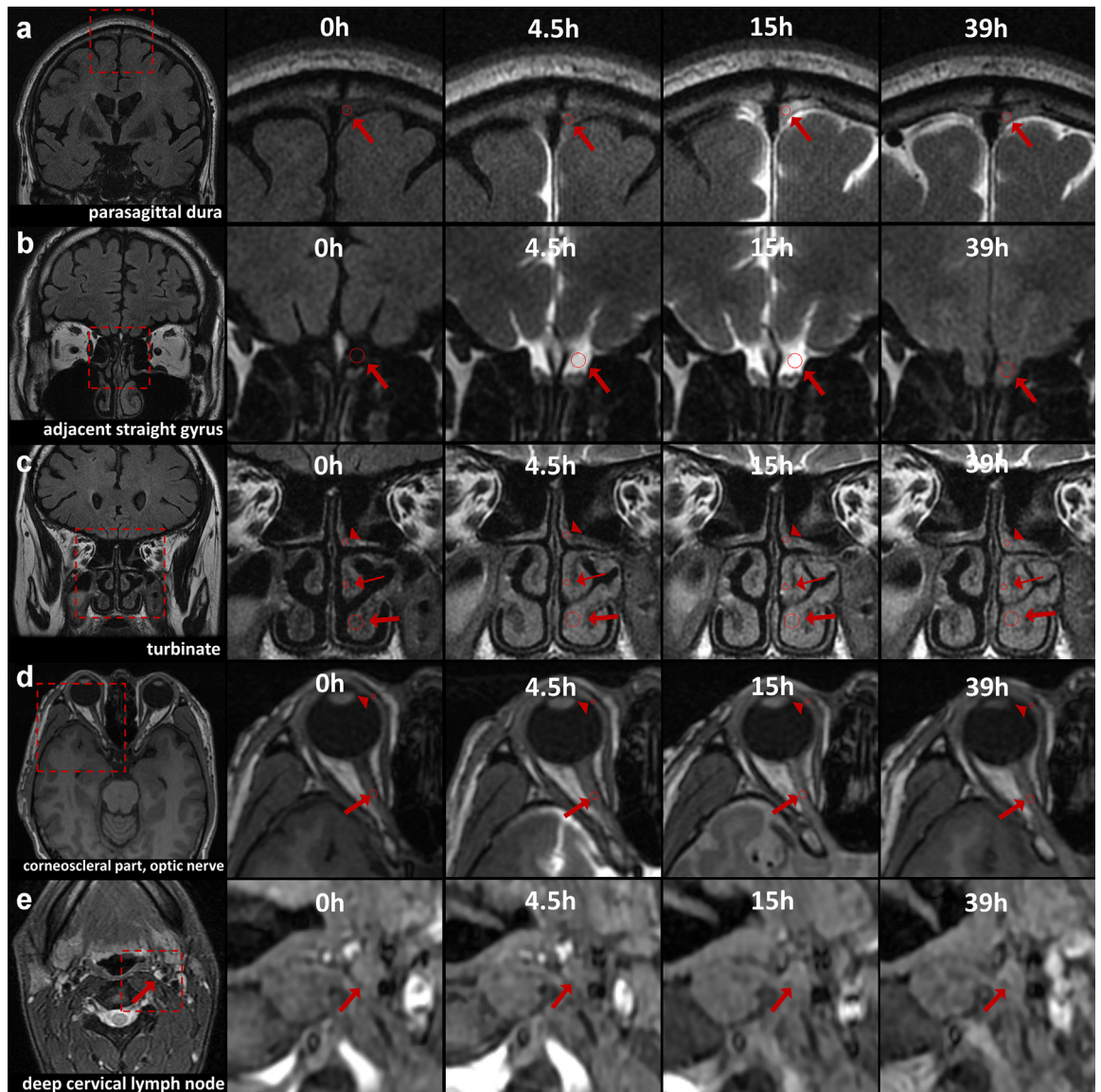
***Fig. 1:* Representative images of meningeal lymphatic and peri-neural pathways and deep cervical lymph nodes.** The clearance of meningeal lymphatic pathway and peri-olfactory nerve pathway on images of head high-resolution 2-dimensional T2-fluid attenuated inversion recovery imaging (a, thick arrow refers to parasagittal dura, b, thick arrow refers to adjacent straight gyrus, c, triangle, thin and thick arrow refer to superior, middle and inferior turbinate, respectively), peri-optic neural pathway on head 3-dimensional T1-weighted imaging (d, triangle and thick arrow refer to corneoscleral part and optic nerve) and deep cervical lymph node on neck T1 fat-suppression imaging (e, thick arrow refers to deep cervical lymph node) are shown, respectively. Each region of interest is indicated by a circle. In each row, The red box on the leftmost image were magnified on the right images and the four images on the right were baseline, 4.5 h images, 15 h images, and 39 h images after the intrathecal administration of gadodiamide, respectively.

mediated by the CSF clearance function. To perform mediation analysis,[18] we tested 3 pathways, that is, step 1, the association of sleep with cognitive function; step 2, the association of sleep with the CSF clearance function; and step 3, the association of the CSF clearance function with cognitive function when controlling for sleep. Multivariable regression analysis was performed for each pathway adjusted for the age, sex, education years and diagnosis of neurodegenerative disease. If all 3 associations are satisfied, the indirect effect was established. The extent of indirect effect is estimated by examining the change in the β of PSQI total scores for T-MoCA total scores before and after including the CSF clearance function. We also adopted

the product of coefficient approach for mediation analysis. We calculated the 95% confidence interval of the indirect effect using bootstrapping technique (5000 replicate samples with replacement). Statistical analyses were performed using the SPSS software version 22.0 (IBM, Armonk, NY). Statistical significance was considered as $P = 0.05$ (2-tailed).

Role of funders
Funding sources of this study had no role in study design, data collection, data analyses, data interpretation, or writing of the manuscript. The corresponding author had full access to all data in this study and had final responsibility for the decision to submit for publication.

Results
Participant characteristics
A total of 92 patients (45 males, mean age = 56 years, age range = 21–85 years; 47 females, mean age = 58 years, age range = 18–79 years) were enrolled. The diagnosis of patients included peripheral neuropathy ($n = 49$), encephalitis ($n = 16$), normal pressure hydrocephalus ($n = 4$), suspected CSF leakage ($n = 4$), hepatic encephalopathy ($n = 1$), possible cerebral amyloid angiopathy ($n = 4$), motor neuron disease ($n = 5$), Parkinson's disease ($n = 5$), multiple system atrophy ($n = 1$), multiple sclerosis ($n = 1$), Alzheimer's disease ($n = 1$), and Lewy body dementia ($n = 1$). T-MoCA scores averaged 14.2 ± 4.3 and PSQI scores averaged 6.7 ± 4.2. Supplementary Table S1 showed the basic clinical data.

Tracer enrichment in all predefined pathways
The ICC of intra-observer and inter-observer consistency for the measurements of the percentage changes in signal unit ratio were 0.831~0.965 and 0.817~0.938, respectively (Supplemental Table S2). In all patients, percentage change in signal unit ratio of parasagittal dura, adjacent straight gyrus, superior turbinate, middle turbinate, inferior turbinate, optic nerve and corneoscleral part significantly altered after the gadolinium injection (Figs. 1 and 2). Our sample size provided enough empirical power to detect significant differences (Supplementary Table S3). We presented the peak time point at each region among all patients (Supplementary Table S4). In summary, the CSF tracer appeared at adjacent straight gyrus before at least one turbinate in 44.2% (23/52) of patients, before at least two turbinates in 32.78% (17/52) of patients and before all turbinates in 23.1% (12/52) of patients. In addition, the tracer appeared at the optic nerve before corneoscleral part in 18.8% (16/85) of patients, at the same time point as corneoscleral part in 70.6% (60/85) of patients, whereas later than corneoscleral part in 10.6% (9/85) of patients.

Additionally, the tracer appeared at the deep cervical lymph node later than parasagittal dura, turbinate, or corneoscleral part in 60.0% (9/15) of patients. Supplementary Table S5 shows the proportion of different peak time points at each region among all patients. The peak time point in the superior, middle and inferior turbinate were significantly later than adjacent straight gyrus (all $P < 0.05$; Paired Samples Wilcoxon Signed Rank Test), but there was no significant difference of peak time point between optic nerve and corneoscleral part ($P = 0.318$; Paired Samples Wilcoxon Signed Rank Test).

Impairment CSF clearance function with ageing
The worse clearance function of parasagittal dura, adjacent straight gyrus, superior turbinate and middle turbinate were significantly related to ageing (all $P < 0.05$; Pearson Correlation Test; Fig. 3). However, no significant correlations were found between the clearance function of inferior turbinate, optic nerve and corneoscleral part with aging (all $P > 0.05$; Pearson Correlation Test; Fig. 3). In addition, when age, sex and diagnosis of neurodegenerative disease were entered as independent variables in linear regression, ageing was still significantly associated with the worse clearance function of the parasagittal dura, adjacent straight gyrus, superior turbinate and middle turbinate ($\beta = 0.046$, $P = 0.001$; $\beta = 0.145$, $P = 0.002$; $\beta = 0.006$, $P = 0.004$; $\beta = 0.004$, $P = 0.041$; Linear Regression Analysis). The representative images in Fig. 4 showed the relationship between the clearance function of parasagittal dura, superior turbinate, middle turbinate and inferior turbinate with ageing.

Relationship between CSF clearance and cognitive function
The clearance function of superior turbinate, middle, and inferior turbinates were all positively related to T-MoCA total scores (all FDR $P < 0.05$; Pearson Correlation Test; Table 1). After adjusting for age, sex, education years and diagnosis of neurodegenerative diseases, the clearance function of superior, middle turbinate and inferior turbinates were independent protective factors of T-MoCA total scores ($\beta = -5.027$, $P = 0.039$; $\beta = -7.625$, $P = 0.003$; $\beta = -6.552$, $P = 0.002$; Linear Regression Analysis). In the subgroup of peripheral neuropathy ($n = 35$), the clearance function of middle turbinate was positively related to T-MoCA total scores ($P = 0.009$; Pearson Correlation Test; Supplementary Table S6). For the sub-item of T-MoCA, the clearance function of middle turbinate was positively correlated with orientation (FDR $P = 0.042$; Pearson Correlation Test; Table 1). However, no significant relationships were found between T-MoCA scores and the clearance function of parasagittal dura, adjacent straight
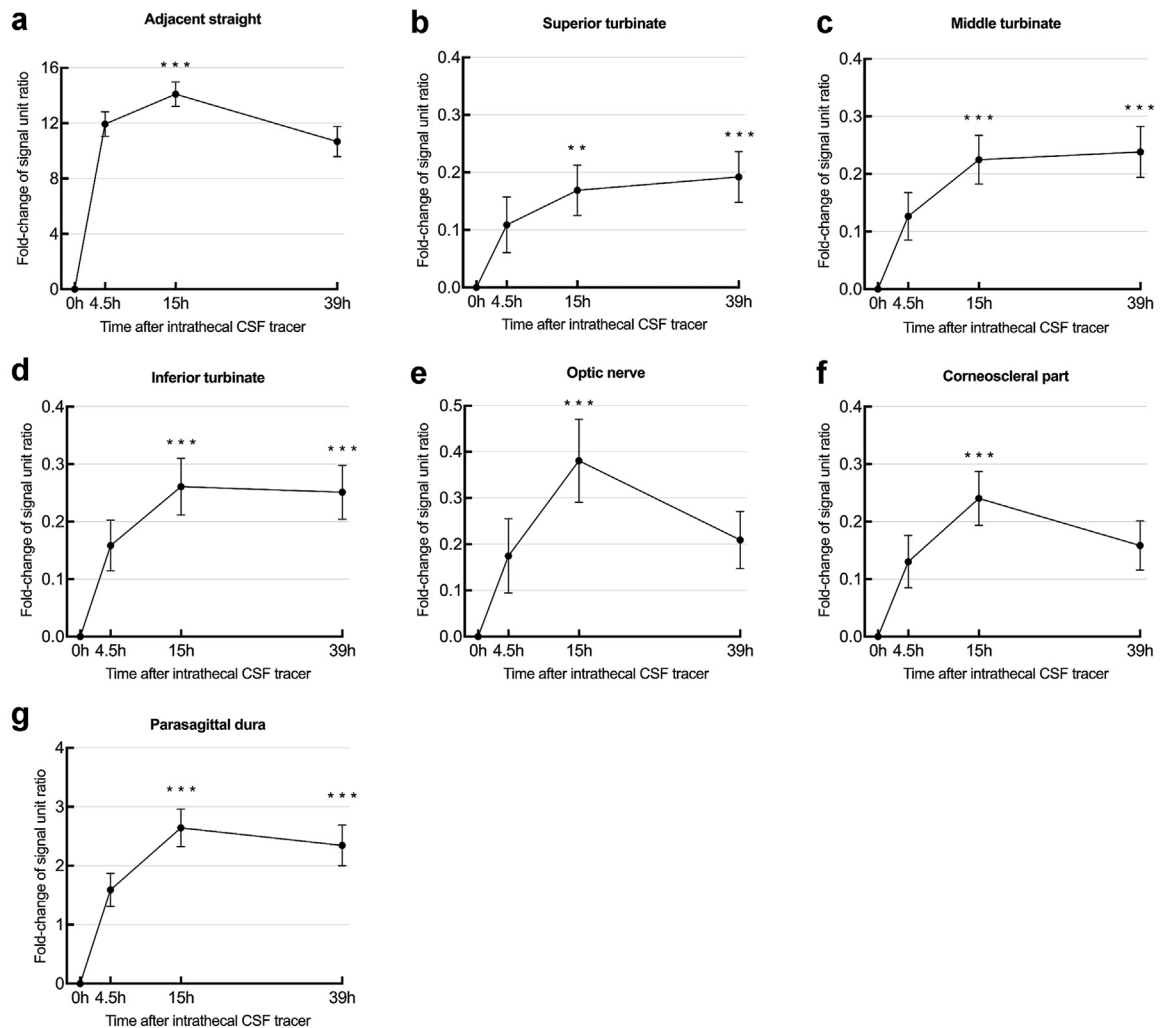
Fig. 2: Tracer enrichment in different locations. The fold-change of signal unit ratio from baseline to 4.5, 15, and 39 h after CSF tracer administration through adjacent straight gyrus (a), superior turbinate (b), middle turbinate (c), inferior turbinate (d), optic nerve (e), corneoscleral part (f), and parasagittal dura (g). Error bars refer to 95% confidence interval. The stars indicated the significant differences compared to 4.5 h by linear mixed model analysis; **$P < 0.01$, ***$P < 0.001$.

gyrus, optic nerve, and corneoscleral part (all $P > 0.05$; Pearson Correlation Test; Table 1).

Relationship between CSF clearance and dyssomnia
The clearance function of superior, middle, and inferior turbinate was all negatively correlated with the PSQI total, while the clearance function of inferior turbinate additionally correlated with sleep quality, and the clearance function of middle turbinate further correlated with sleep quality and sleep latency (all FDR $P < 0.05$; Spearman Correlation Test; Table 2). No significant relationship was found between PSQI scores and the clearance function of parasagittal dura, adjacent straight gyrus, corneoscleral part and optic nerve (all $P > 0.05$; Spearman Correlation Test; Table 2). After adjusting for

age, sex and diagnosis of neurodegenerative diseases, the PSQI total scores was independently associated with the clearance function of middle turbinate and inferior turbinate ($\beta = 0.012$, $P = 0.032$; $\beta = 0.016$, $P = 0.014$; Linear Regression Analysis). In the subgroup of peripheral neuropathy ($n = 35$), the clearance function of middle and inferior turbinate were negatively correlated to PSQI total scores ($P = 0.013$; $P = 0.006$; Spearman Correlation Test; Supplementary Table S6).

Mediation of CSF clearance in the association of dyssomnia with cognitive decline
In 75 patients who completed 2-dimensional T2-fluid attenuated inversion recovery at 39 h, 19 subjects did not perform the PSQI tests and 2 subjects did not
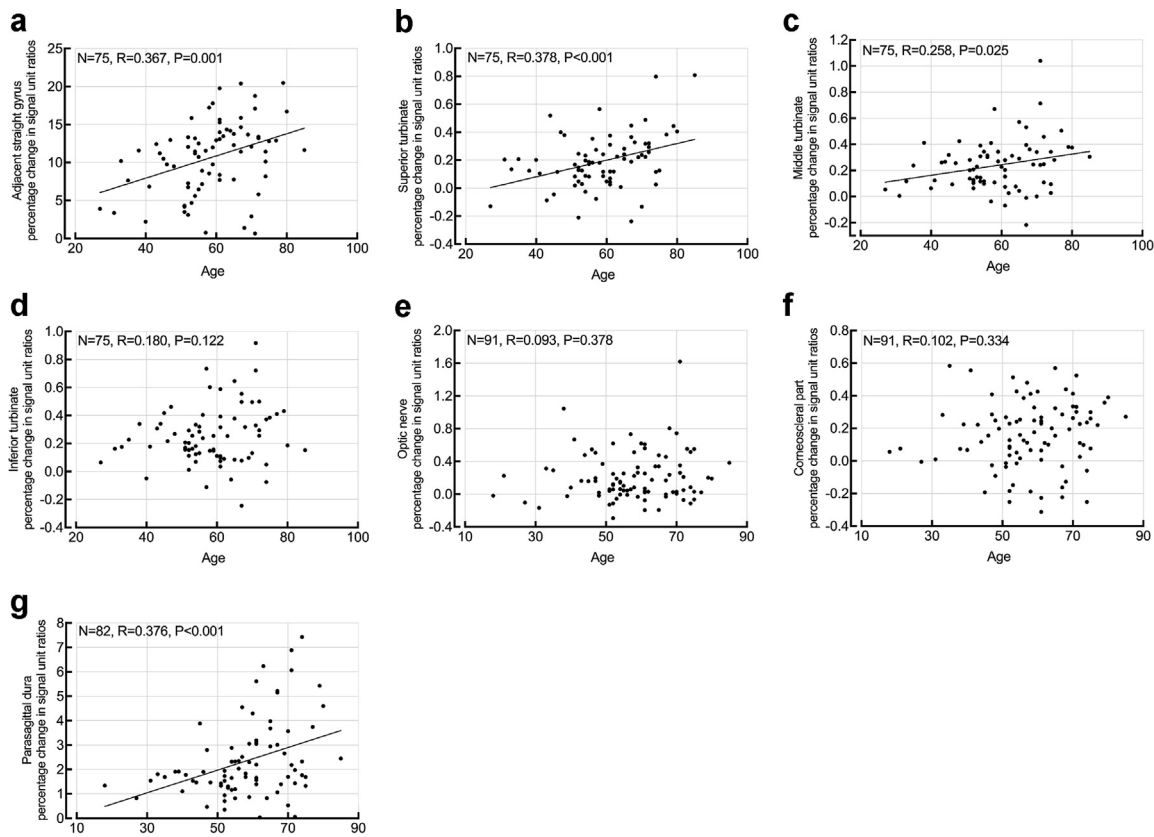
Fig. 3: Correlations between age and the clearance function on the seven predefined locations. There was a positive correlation between age and the clearance function through adjacent straight gyrus (a), superior turbinate (b), middle turbinate (c), or parasagittal dura (g), respectively. No significant correlation was observed in the clearance of inferior turbinate (d), optic nerve (e), and corneoscleral part (f) with age. Each plot shows the sample size, fit line, and the Pearson correlation coefficient (r) with P-value.

complete T-MoCA test, leaving 54 patients for final analysis. Supplementary Table S7 showed their basic clinical data. In the adjusted model, the PSQI total scores was negatively associated with the T-MoCA total scores (β = −0.252, P = 0.014; Linear Regression Analysis; Table 3). When age, sex, education years and diagnosis of neurodegenerative diseases were entered as covariates, the effect size of PSQI total scores on T-MoCA total scores was significantly reduced after controlling for the clearance function of inferior turbinate (change in β [bootstrap 95% confidence interval]: −0.082 [−0.220, −0.007]; Table 3). The clearance function of inferior turbinate, which was mediators, explained 33% of the association between PSQI total scores and T-MoCA total scores. The clearance function of superior and middle turbinate did not significantly mediate the effect of PSQI total scores on T-MoCA total scores (change in β [bootstrap 95% confidence interval]: −0.039 [−0.150, 0.020]; change in β [bootstrap 95% confidence interval]: −0.066 [−0.168, 0.001]).

Discussion

In the current study, we provided a method to simultaneously visualize the CSF clearance through three pathways: meningeal lymphatic pathway, peri-olfactory and peri-optic nerve pathways. The deep cervical lymph nodes were their potential CSF drainage way as the tracer appearance at the deep cervical lymph nodes was later than anyone of above three pathways in 9 of 15 patients. Similar to meningeal lymphatic pathway, the clearance function of peri-olfactory nerve pathway was also impaired with aging. Importantly, CSF clearance function through the peri-olfactory inferior turbinate pathway explained 33% of the association between PSQI total scores and T-MoCA total scores, indicating its potential intervening mechanism involving dyssomnia and cognitive decline.

Rodent studies have proved that the nasal region across the cribriform plate was the main CSF outflow site.[19] Recently, a series of MRI images in mice with contrast agent infused into the lateral ventricle achieved
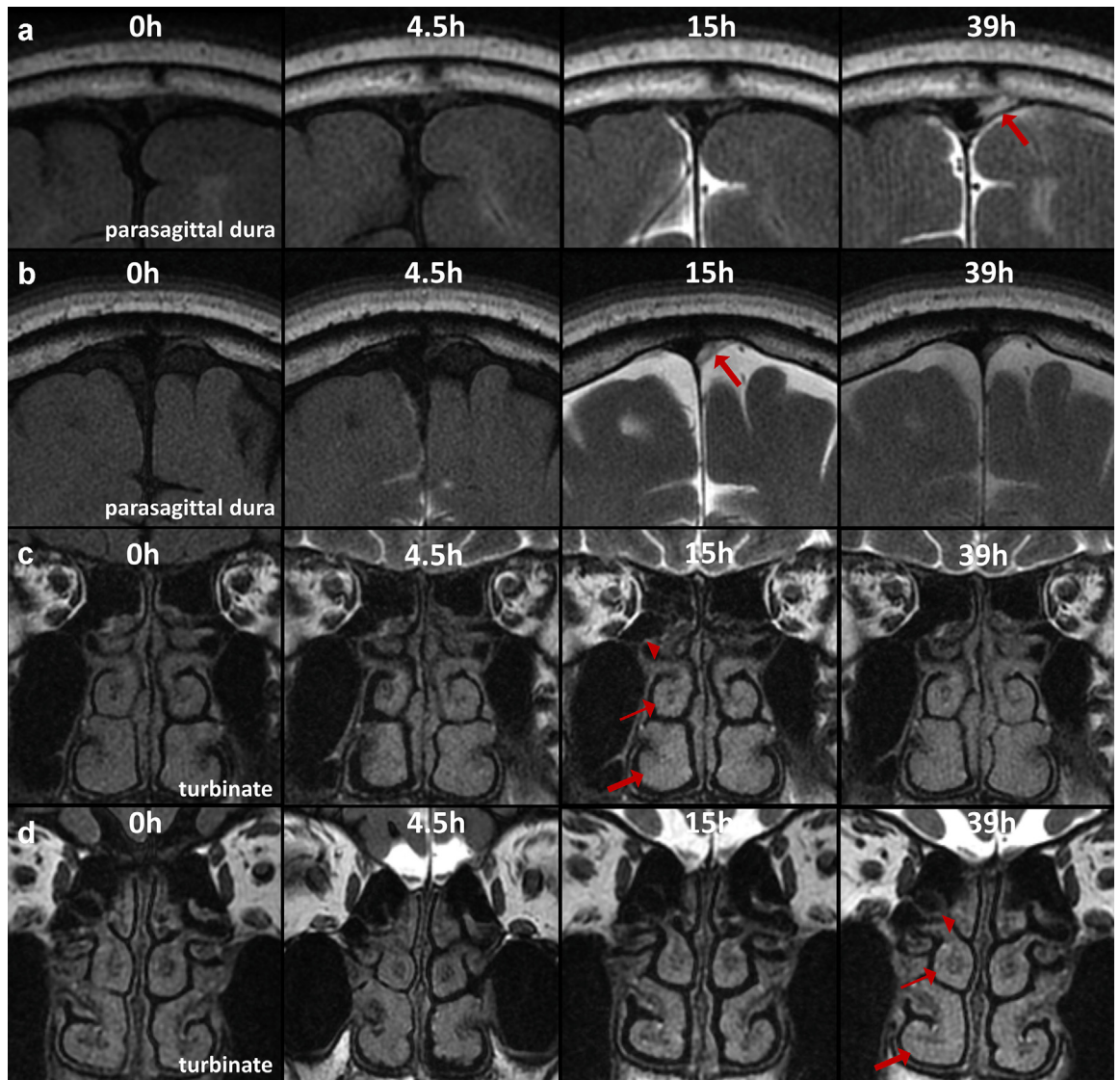
Fig. 4: Representative images show the delayed clearance of the meningeal lymphatic pathway and peri-olfactory nerve pathway in aging patients. From the images of coronal head 2-dimensional T2-fluid attenuated inversion recovery at baseline (0 h), 4.5 h, 15 h, and 39 h after the intrathecal administration of gadodiamide, the signals of parasagittal dura (a and b; arrow) and turbinates (c and d; triangle, thin and thick arrow refer to superior, middle and inferior turbinate, respectively) changed significantly, indicating the CSF clearance through meningeal lymphatic pathway and peri-olfactory nerve pathway. The peak time point of signal unit ratio of parasagittal dura in the 65-year-old patient (at 39 h; a) is later than that in the 31-year-old patient (at 15 h; b), and the peak time point of signal unit ratio of turbinate in the 79-year-old patient (at 39 h; c) is later than that in the 54-year-old patient (at 15 h; d).

a 3D dynamic visualization of the CSF drainage, revealing a continuous anatomic route from the region of the olfactory bulbs to the nasopharynx and the deep cervical lymph nodes.[20] Human post-mortem were also observed that Microfil dye injected into the CSF compartment located primarily in the subarachnoid space around the olfactory bulbs and cribriform plate.[21] Our findings indicated possible drainage of CSF to the turbinates via the cribriform plate along olfactory nerve in human. This finding is in line with previous results from PET studies.[12] In another MRI study with intrathecal injection of tracer, although the significant change of signal intensity over time in the nasal turbinates was not observed, contrast agent was observable in almost half of the patients below the cribriform plate along the olfactory nerves.[13] The relatively large sample size in our study have increased the statistical power. Further studies with larger sample size and

	T-MoCA total scores	Attention and calculation	Language	Abstraction	Delayed recall	Orientation
Parasagittal dura (n = 57)						
R	−0.125	−0.048	−0.140	−0.092	−0.080	−0.093
FDR P	0.621	0.846	0.382	0.579	0.646	0.690
Adjacent straight gyrus (n = 54)						
R	−0.062	0.023	−0.149	−0.102	0.019	−0.096
FDR P	0.765	0.869	0.382	0.579	0.893	0.690
Superior turbinate (n = 54)						
R	−0.379	−0.287	−0.136	−0.129	−0.345	−0.275
FDR P	0.012	0.082	0.382	0.579	0.077	0.110
Middle turbinate (n = 54)						
R	−0.449	−0.359	−0.321	−0.304	−0.213	−0.368
FDR P	0.007	0.056	0.063	0.175	0.273	0.042
Inferior turbinate (n = 54)						
R	−0.397	−0.313	−0.328	−0.258	−0.205	−0.272
FDR P	0.011	0.074	0.063	0.210	0.273	0.110
Optic nerve (n = 59)						
R	−0.089	0.069	−0.174	0.070	−0.187	−0.025
FDR P	0.707	0.846	0.382	0.598	0.273	0.850
Corneoscleral part (n = 59)						
R	0.020	−0.063	−0.021	0.093	0.128	−0.067
FDR P	0.882	0.846	0.876	0.579	0.469	0.719

T-MoCA: Telephone Montreal Cognitive Assessment; R: Spearman correlation coefficient; All P value were corrected false discovery rate by the Benjamini-Hochberg method in T-MoCA total scores and each cognitive domain respectively.

Table 1: Correlations between cognitive function and percentage change of signal unit ratios from baseline to 39 h in predefined seven locations.

homogeneous participants are needed to get a better understanding towards this discrepancy. Interestingly, we only found a very slight enhancement of the nasal turbinates after intrathecal injection, which is similar to a previous rodent study.[20] The contrast agent was infused into the lateral ventricle in mice and the MRI images showed that only a minimal increase of signal could be detected within the turbinates, whereas much larger signal increases were detected at the nasopharynx. Histological sections after ovalbumin infusion show that the tracer spread throughout a wide volume of nasal tissue after crossing cribriform plate, which may partially account for the very slight enhancement of nasal turbinates in humans with MRI.

The three-layer sheath of the optic nerve continues with the meninges, with the dura mater and the arachnoid membrane fusing with the sclera at the distal end of the optic nerve.[22] Lüdemann et al. observed that the arachnoid barrier layer was not continuous at the termination of the optic nerve and an outflow of tracer occurred in cat.[23] Tracer was also found in the conjunctival lymphatics. Rodent study observed a dense plexus of tracer-filled lymphatic in the connective tissue beside the eyeball, and these lymphatics merged into a collecting vessel, tracking alongside the anterior facial vein to the mandibular lymph nodes.[5] In the current study, we directly observed that the signal intensities both in middle intraorbital segment of the optic nerve

and corneoscleral part changed over time, providing further evidence for the clearance of CSF through peri-optic nerve pathway. In addition, we found that in 89.4% patients, the tracer appeared at optic nerve before or at the same time point as corneoscleral part, but there was no significant difference in the peak time point of the tracer in these two regions. We speculated that CSF might drain to the corneoscleral part via peri-optic space. However, it was not confirmed in our images possibly due to relatively long scan interval. Further study with more observation time points and higher resolution MRI imaging is strongly needed to clarify this specific pathway.

In most patients (9/15), the tracer appeared at deep cervical lymph nodes after meningeal lymphatic pathway, peri-olfactory or peri-optic nerve pathways, supporting the potential drainage of CSF to deep cervical lymph node from cranium.[17,24] The individual differences in the clearance might explain the unexpected results in the remaining 3 patients, as a certain pathway in some patients might contribute little to the overall CSF draining, which could not alter the peak time of deep cervical lymph node.

Multiple animal studies have demonstrated that CSF clearance function decrease with ageing.[5,10,25] Our previous study also found that the meningeal lymphatic pathway was impaired in ageing human.[10] In the current study, we once again confirmed this conclusion with a

	PSQI total scores	Sleep quality	Sleep latency	Sleep duration	Habitual sleep efficiency	Sleep disturbances	Use of sleeping medication	Daytime dysfunction
Parasagittal dura (n = 60)								
ρ	0.091	0.037	0.176	0.003	0.025	–0.062	0.094	–0.019
FDR P	0.571	0.908	0.312	0.982	0.853	0.849	0.828	0.893
Adjacent straight gyrus (n = 56)								
ρ	–0.028	0.004	–0.109	–0.122	–0.116	–0.031	0.125	0.034
FDR P	0.836	0.977	0.492	0.482	0.459	0.849	0.828	0.893
Superior turbinate (n = 56)								
ρ	0.330	0.252	0.216	0.289	0.253	0.057	–0.007	0.225
FDR P	0.030	0.107	0.254	0.217	0.140	0.849	0.958	0.224
Middle turbinate (n = 56)								
ρ	0.433	0.333	0.439	0.215	0.191	0.044	–0.025	0.300
FDR P	0.007	0.042	0.007	0.235	0.272	0.849	0.958	0.158
Inferior turbinate (n = 56)								
ρ	0.401	0.390	0.321	0.203	0.176	–0.092	0.129	0.269
FDR P	0.007	0.021	0.056	0.235	0.272	0.849	0.828	0.158
Optic nerve (n = 62)								
ρ	0.133	0.199	0.116	0.200	0.246	0.025	–0.152	–0.042
FDR P	0.426	0.171	0.492	0.235	0.140	0.849	0.828	0.893
Corneoscleral part (n = 62)								
ρ	0.216	0.270	0.028	0.106	0.307	0.099	–0.021	0.157
FDR P	0.161	0.079	0.826	0.482	0.105	0.849	0.958	0.439

PSQI: Pittsburgh Sleep Quality Index. ρ: Pearson correlation coefficient; All P value were corrected false discovery rate by the Benjamini-Hochberg method in PSQI total scores and each domain respectively.

Table 2: **Correlations between sleep quality and percentage change of signal unit ratios from baseline to 39 h in predefined seven locations.**

larger sample size. Meanwhile, the similar relationship was also found in the peri-olfactory nerve pathway, which was accordant with the animal finding that less CSF drain to the nasal turbinates in aged mice.[19,26] Especially in an MRI study,[20] they found slower dynamics of CSF clearance and transport at nasal turbinates and nasopharyngeal lymphatics in older mice, which is consistent with our finding. In our study, reduced clearance of the peri-optic nerve pathway with ageing was not found. This indicates that the changes in the CSF clearance with ageing may be inconsistent in different pathways. Excitingly, we demonstrated that the

dysfunction of CSF clearance from peri-olfactory nerve pathway was related to cognitive impairment. This finding is of great importance, as olfactory dysfunction is an important early manifestation in several neurodegenerative diseases such as Alzheimer's disease.[27] The pathological changes of Alzheimer's disease widely emerge in the regions involved in olfactory information processing from the peripheral olfactory epithelium to the central entorhinal cortex prior to the symptomatic onset of cognitive impairment.[28,29] Additionally, the odour identification performance is highly correlated with hippocampal volume in Alzheimer's disease

Pathway	Unadjusted				Adjusted			
	B	95% CI		P	β	95% CI		P
a	0.016	0.004	0.028	0.012	0.015	0.002	0.028	0.025
b	–6.400	–12.018	–0.782	0.026	–5.422	–9.542	–1.303	0.011
c	–0.391	–0.648	–0.133	0.004	–0.252	–0.450	–0.055	0.014
c′	–0.288	–0.552	–0.024	0.033	–0.170	–0.367	0.026	0.088

a, The regression coefficient of the association of Sleep Quality Index (PSQI) total scores with the clearance function of inferior turbinate; b, the regression coefficient of association of the clearance function of inferior turbinate with Telephone Montreal Cognitive Assessment (T-MoCA) total scores, controlling for PSQI total scores; c, the regression coefficient of association of PSQI total scores with T-MoCA total scores; and c′, the regression coefficient of association of PSQI total scores with T-MoCA total scores, controlling for the clearance function of inferior turbinate. Multivariable regression analysis for each pathway adjusted for the age, sex, education years and diagnosis of neurodegenerative disease.

Table 3: **Association of sleep quality with cognitive function mediated by the percentage change of signal unit ratios from baseline to 39 h in inferior turbinate.**

patients.[30] Impaired peri-olfactory nerve pathway, associated with early olfactory dysfunction, may lead to the continuous deposition of abnormal protein and subsequent cognitive dysfunction. The predictive value of peri-olfactory nerve pathway on cognitive function may be worthwhile to test in different diseases.

The evidence for the relationship between CSF draining pathway and sleep in human is still limited. Interestingly, we found the impaired drainage of peri-olfactory nerve pathway, but unchanged drainage of parasagittal dura in patients with chronic sleep disorders. Previously, unchanged tracer enrichment in parasagittal dura after total sleep deprivation of one night was also found,[31] suggesting that molecular egress to parasagittal dura might be independent of acute or chronic sleep deprivation. Importantly, our further mediation analysis explained that impaired drainage of peri-olfactory nerve pathway might play an important role in the cognitive decline in patients with chronic sleep disorders, which also lends support to the connection between dyssomnia and cognitive impairment.[32] Poor sleep quality increased amyloid β burden and promoted neuroinflammation, especially in hippocampal areas, resulting in cognitive impairment.[33,34] Our findings thus provide evidence that peri-olfactory CSF clearance may be the important pathway for the drainage of abnormal proteins and inflammatory molecules in patient with poor sleep. This finding would have great clinical implication, as improving CSF clearance of peri-olfactory nerve via nasal drug delivery system, which bypasses the blood–brain barrier and has good patient compliance, may have potential for the intervention of dementia.[35] Although mediation analysis were performed in cross-sectional studies and the causality cannot be ascertained, these findings can still provide the groundwork for alternative designs, such as interventional experiments and longitudinal designs for further verification.

Our research has several limitations. First, the identification of meningeal lymphatic and peri-neural pathways were based on MRI and lacking corresponding pathological evidence. Second, both cognitive decline and sleep quality were assessed by surveys rather than measured with a more robust manner, thus more professional tests and cohort design are needed to confirm the phenomenon. In addition, the ROIs in current study were manually placed, which might bring some measurement errors, although the consistency of the image evaluation between different observers is relatively high. Third, our study included a wide range of patients with different diseases, such as chronic disease including hypertension and diabetes, which could affect the clearance function of these pathways. Although we entered the diagnosis of neurodegenerative disease as covariates in the relative analysis and performed subgroup analyses in peripheral neuropathy group, the results on age, cognitive function and sleep

variation should also be interpreted with caution. Moreover, we enrolled patients needing CSF examination who might not be representative of the general population with dyssomnia. Therefore, studies in the specific population are needed. Fourth, we only obtained images at 3 time points after the intrathecal injection of the contrast agent with relatively long interval, which might not be sufficient for timing relationship among different locations. The clearance function of the CSF tracer, which was actually a dynamic process, was simply regarded as the retention of tracer at 39 h in the prespecified regions. Further studies with additional time points would help understand the dynamic process of tracer clearance in more details.

In conclusion, this study provides in-vivo evidence of CSF clearance through meningeal lymphatic pathway, peri-olfactory and peri-optic nerve pathway in human and shows promise for dynamic MRI with intrathecal injection of contrast agent as a method to assess CSF clearance function through these pathways. This study also interprets the impaired peri-olfactory nerve clearance underlying the cognitive decline in patients with dyssomnia and indicates that it may be an important pathway for the drainage of abnormal proteins and inflammatory molecules in patients with poor sleep quality.

References
1 Spector R, Robert Snodgrass S, Johanson CE. A balanced view of the cerebrospinal fluid composition and functions: focus on adult humans. *Exp Neurol*. 2015;273:57–68. https://doi.org/10.1016/j.expneurol.2015.07.027.
2 Pollay M. The function and structure of the cerebrospinal fluid outflow system. *Cerebrospinal Fluid Res*. 2010;7:9. https://doi.org/10.1186/1743-8454-7-9.

3 Proulx ST. Cerebrospinal fluid outflow: a review of the historical and contemporary evidence for arachnoid villi, perineural routes, and dural lymphatics. *Cell Mol Life Sci.* 2021;78(6):2429–2457. https://doi.org/10.1007/s00018-020-03706-5.

4 Kaur J, Fahmy LM, Davoodi-Bojd E, et al. Waste clearance in the brain. *Front Neuroanat.* 2021;15:665803. https://doi.org/10.3389/fnana.2021.665803.

5 Ma Q, Ineichen BV, Detmar M, Proulx ST. Outflow of cerebrospinal fluid is predominantly through lymphatic vessels and is reduced in aged mice. *Nat Commun.* 2017;8:1434. https://doi.org/10.1038/s41467-017-01484-6.

6 Da Mesquita S, Louveau A, Vaccari A, et al. Functional aspects of meningeal lymphatics in ageing and Alzheimer's disease. *Nature.* 2018;560(7717):185–191. https://doi.org/10.1038/s41586-018-0368-8.

7 Hablitz LM, Plá V, Giannetto M, et al. Circadian control of brain glymphatic and lymphatic fluid flow. *Nat Commun.* 2020;11:4411. https://doi.org/10.1038/s41467-020-18115-2.

8 Ma Q, Ries M, Decker Y, et al. Rapid lymphatic efflux limits cerebrospinal fluid flow to the brain. *Acta Neuropathol.* 2019;137(1):151–165. https://doi.org/10.1007/s00401-018-1916-x.

9 Absinta M, Ha SK, Nair G, et al. Human and nonhuman primate meninges harbor lymphatic vessels that can be visualized non-invasively by MRI. *Elife.* 2017;6:e29738. https://doi.org/10.7554/eLife.29738.

10 Zhou Y, Cai J, Zhang W, et al. Impairment of the glymphatic pathway and putative meningeal lymphatic vessels in the aging human. *Ann Neurol.* 2020;87(3):357–369. https://doi.org/10.1002/ana.25670.

11 Ringstad G, Eide PK. Cerebrospinal fluid tracer efflux to parasagittal dura in humans. *Nat Commun.* 2020;11(1):354. https://doi.org/10.1038/s41467-019-14195-x.

12 de Leon MJ, Li Y, Okamura N, et al. Cerebrospinal fluid clearance in Alzheimer disease measured with dynamic PET. *J Nucl Med.* 2017;58(9):1471–1476. https://doi.org/10.2967/jnumed.116.187211.

13 Melin E, Eide PK, Ringstad G. In vivo assessment of cerebrospinal fluid efflux to nasal mucosa in humans. *Sci Rep.* 2020;10(1):14974. https://doi.org/10.1038/s41598-020-72031-5.

14 Fahmy LM, Chen Y, Xuan S, Haacke EM, Hu J, Jiang Q. All central nervous system neuro- and vascular-communication channels are surrounded with cerebrospinal fluid. *Front Neurol.* 2021;12:614636. https://doi.org/10.3389/fneur.2021.614636.

15 Buysse DJ, Reynolds CF, Monk TH, Berman SR, Kupfer DJ. The Pittsburgh Sleep Quality Index: a new instrument for psychiatric practice and research. *Psychiatry Res.* 1989;28(2):193–213. https://doi.org/10.1016/0165-1781(89)90047-4.

16 Pendlebury ST, Welch SJV, Cuthbertson FC, Mariz J, Mehta Z, Rothwell PM. Telephone assessment of cognition after transient ischemic attack and stroke: modified telephone interview of cognitive status and telephone Montreal Cognitive Assessment versus face-to-face Montreal Cognitive Assessment and neuropsychological battery. *Stroke.* 2013;44(1):227–229. https://doi.org/10.1161/STROKEAHA.112.673384.

17 Eide PK, Vatnehol SAS, Emblem KE, Ringstad G. Magnetic resonance imaging provides evidence of glymphatic drainage from human brain to cervical lymph nodes. *Sci Rep.* 2018;8(1):7194. https://doi.org/10.1038/s41598-018-25666-4.

18 Baron RM, Kenny DA. The moderator-mediator variable distinction in social psychological research: conceptual, strategic, and statistical considerations. *J Pers Soc Psychol.* 1986;51(6):1173–1182. https://doi.org/10.1037//0022-3514.51.6.1173.

19 Brady M, Rahman A, Combs A, et al. Cerebrospinal fluid drainage kinetics across the cribriform plate are reduced with aging. *Fluids Barriers CNS.* 2020;17:71. https://doi.org/10.1186/s12987-020-00233-0.

20 Decker Y, Krämer J, Xin L, et al. Magnetic resonance imaging of cerebrospinal fluid outflow after low-rate lateral ventricle infusion in mice. *JCI Insight.* 2022;7(3):e150881. https://doi.org/10.1172/jci.insight.150881.

21 Johnston M, Zakharov A, Papaiconomou C, Salmasi G, Armstrong D. Evidence of connections between cerebrospinal fluid and nasal lymphatic vessels in humans, non-human primates and other mammalian species. *Cerebrospinal Fluid Res.* 2004;1(1):2. https://doi.org/10.1186/1743-8454-1-2.

22 Rodriguez-Peralta LA. Hematic and fluid barriers in the optic nerve. *J Comp Neurol.* 1966;126(1):109–121. https://doi.org/10.1002/cne.901260109.

23 Lüdemann W, Berens von Rautenfeld D, Samii M, Brinker T. Ultrastructure of the cerebrospinal fluid outflow along the optic nerve into the lymphatic system. *Childs Nerv Syst.* 2005;21(2):96–103. https://doi.org/10.1007/s00381-004-1040-1.

24 Louveau A, Smirnov I, Keyes TJ, et al. Structural and functional features of central nervous system lymphatic vessels. *Nature.* 2015;523(7560):337–341. https://doi.org/10.1038/nature14432.

25 Ahn JH, Cho H, Kim JH, et al. Meningeal lymphatic vessels at the skull base drain cerebrospinal fluid. *Nature.* 2019;572(7767):62–66. https://doi.org/10.1038/s41586-019-1419-5.

26 Nagra G, Johnston MG. Impact of ageing on lymphatic cerebrospinal fluid absorption in the rat. *Neuropathol Appl Neurobiol.* 2007;33(6):684–691. https://doi.org/10.1111/j.1365-2990.2007.00857.x.

27 Doty RL. Olfactory dysfunction in neurodegenerative diseases: is there a common pathological substrate? *Lancet Neurol.* 2017;16(6):478–488. https://doi.org/10.1016/S1474-4422(17)30123-0.

28 Murphy C. Olfactory and other sensory impairments in Alzheimer disease. *Nat Rev Neurol.* 2019;15(1):11–24. https://doi.org/10.1038/s41582-018-0097-5.

29 Albers MW, Gilmore GC, Kaye J, et al. At the interface of sensory and motor dysfunctions and Alzheimer's disease. *Alzheimers Dement.* 2015;11(1):70–98. https://doi.org/10.1016/j.jalz.2014.04.514.

30 Murphy C, Jernigan TL, Fennema-Notestine C. Left hippocampal volume loss in Alzheimer's disease is reflected in performance on odor identification: a structural MRI study. *J Int Neuropsychol Soc.* 2003;9(3):459–471. https://doi.org/10.1017/S1355617703930116.

31 Eide PK, Ringstad G. Cerebrospinal fluid egress to human parasagittal dura and the impact of sleep deprivation. *Brain Res.* 2021;1772:147669. https://doi.org/10.1016/j.brainres.2021.147669.

32 Yaffe K, Falvey CM, Hoang T. Connections between sleep and cognition in older adults. *Lancet Neurol.* 2014;13(10):1017–1028. https://doi.org/10.1016/S1474-4422(14)70172-3.

33 Kang JE, Lim MM, Bateman RJ, et al. Amyloid-beta dynamics are regulated by orexin and the sleep-wake cycle. *Science.* 2009;326(5955):1005–1007. https://doi.org/10.1126/science.1180962.

34 Zhu B, Dong Y, Xu Z, et al. Sleep disturbance induces neuroinflammation and impairment of learning and memory. *Neurobiol Dis.* 2012;48(3):348–355. https://doi.org/10.1016/j.nbd.2012.06.022.

35 Khan AR, Liu M, Khan MW, Zhai G. Progress in brain targeting drug delivery system by nasal route. *J Control Release.* 2017;268:364–389. https://doi.org/10.1016/j.jconrel.2017.09.001.